# A Novel Curcumin-Artemisinin Coamorphous Solid: Physical Properties and Pharmacokinetic Profile†

**Kuthuru Suresh,[a] M. K. Chaitanya Mannava,[b] and Ashwini Nangia*[,a,b]**

[a] School of Chemistry, University of Hyderabad, Prof. C. R. Rao Road, Gachibowli, Central University P.O., Hyderabad 500 046, India.
[b] Technology Business Incubator, University of Hyderabad, Prof. C. R. Rao Road, Gachibowli, Central University P.O., Hyderabad 500 046, India.
ashwini.nangia@gmail.com

## Electronic Supplementary Information†

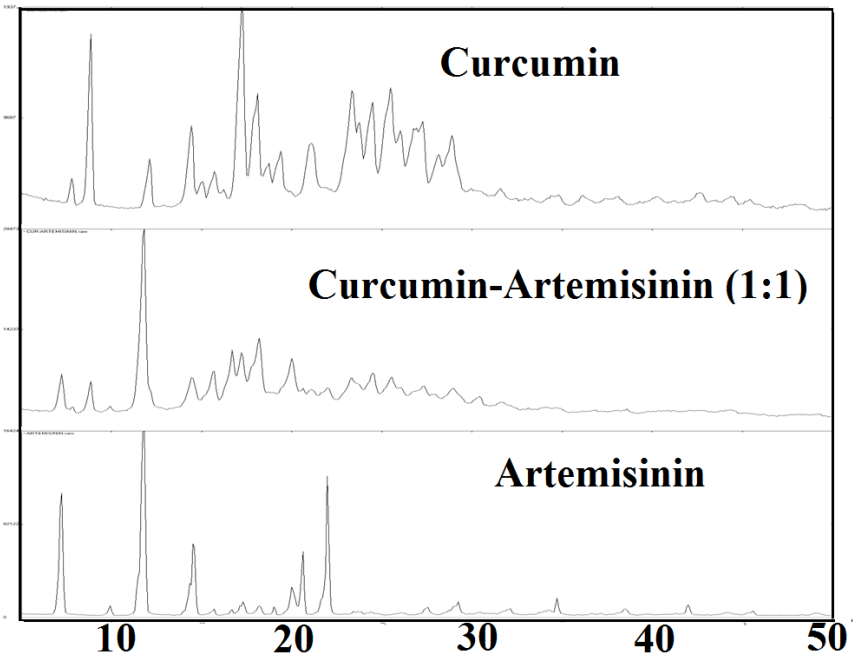


**Figure S1a** Curcumin-Artemisinin (1:1) solvent (EtOH) assisted grinding PXRD pattern comparison with starting materials.

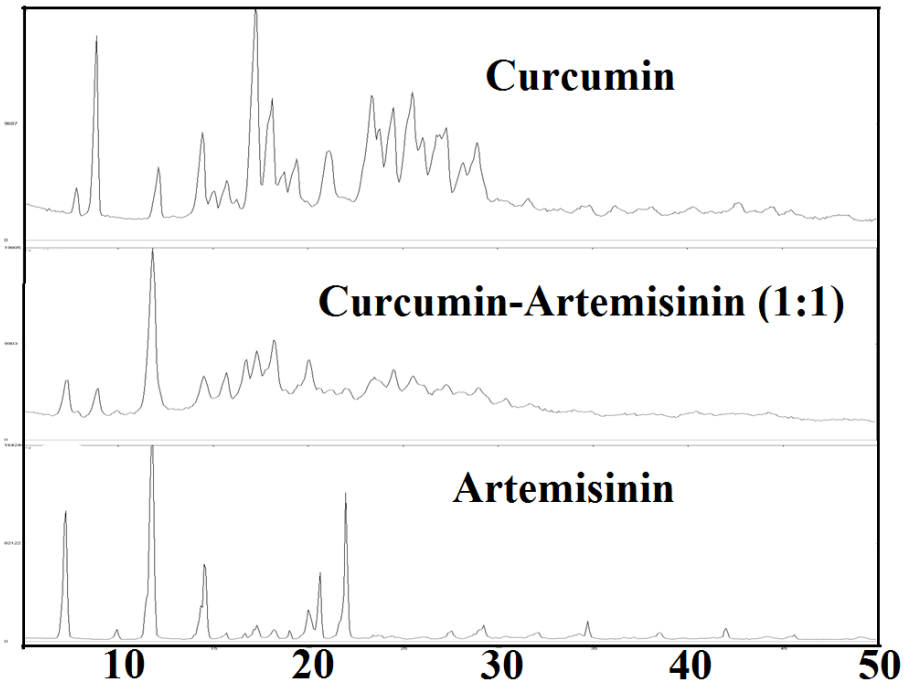


**Figure S1b** Curcumin-Artemisinin (1:1) ball mill grinding PXRD pattern comparison with starting materials.

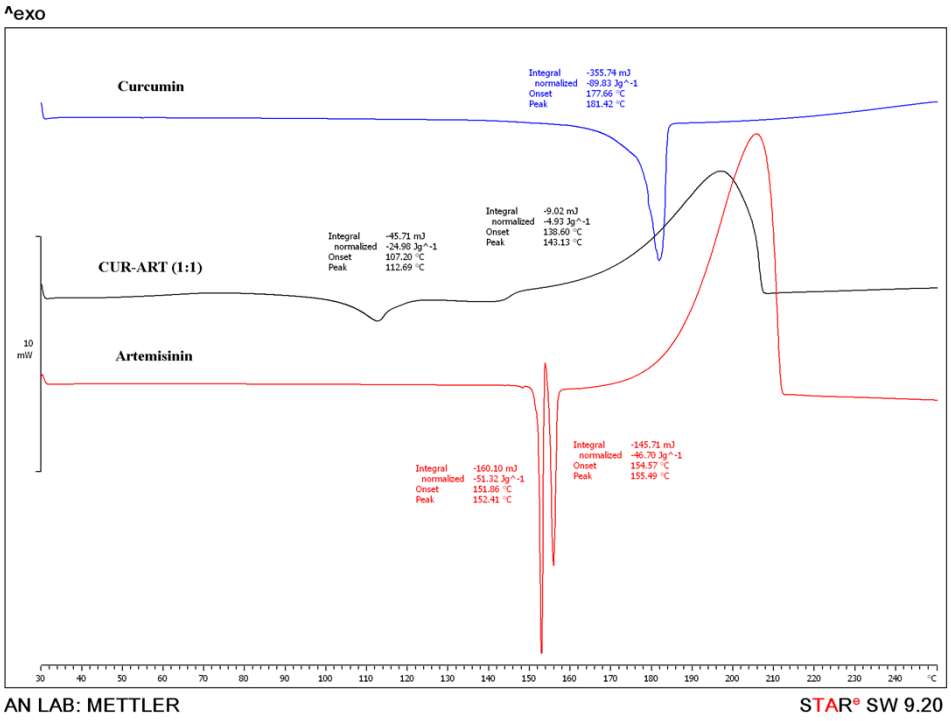


**Figure S2** DSC heating curve of Curcumin-Artemisinin (1:1) (prepared by ball mill grinding) comparison with starting materials.

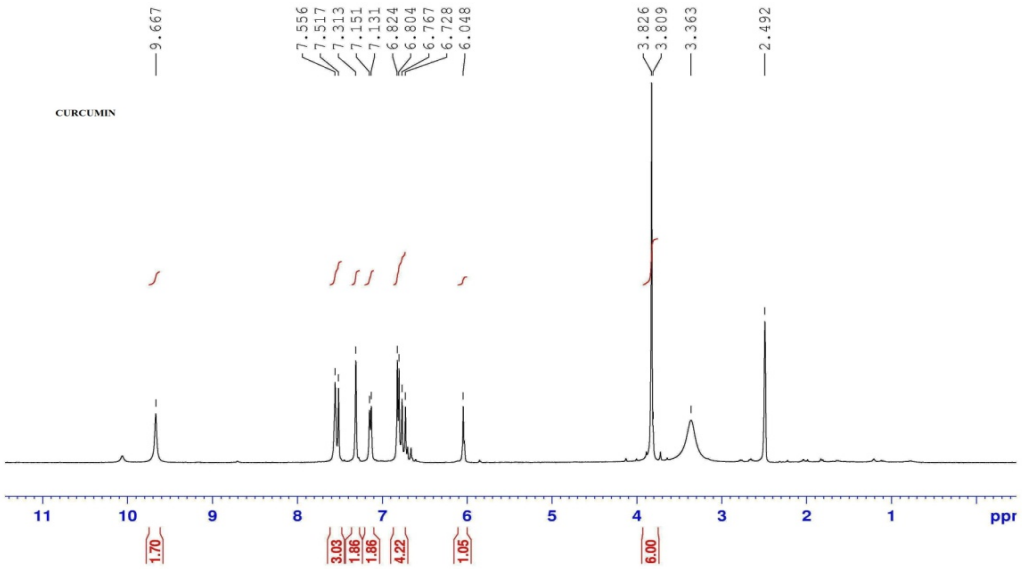


**Figure S3a** [1]H NMR spectrum of Curcumin.

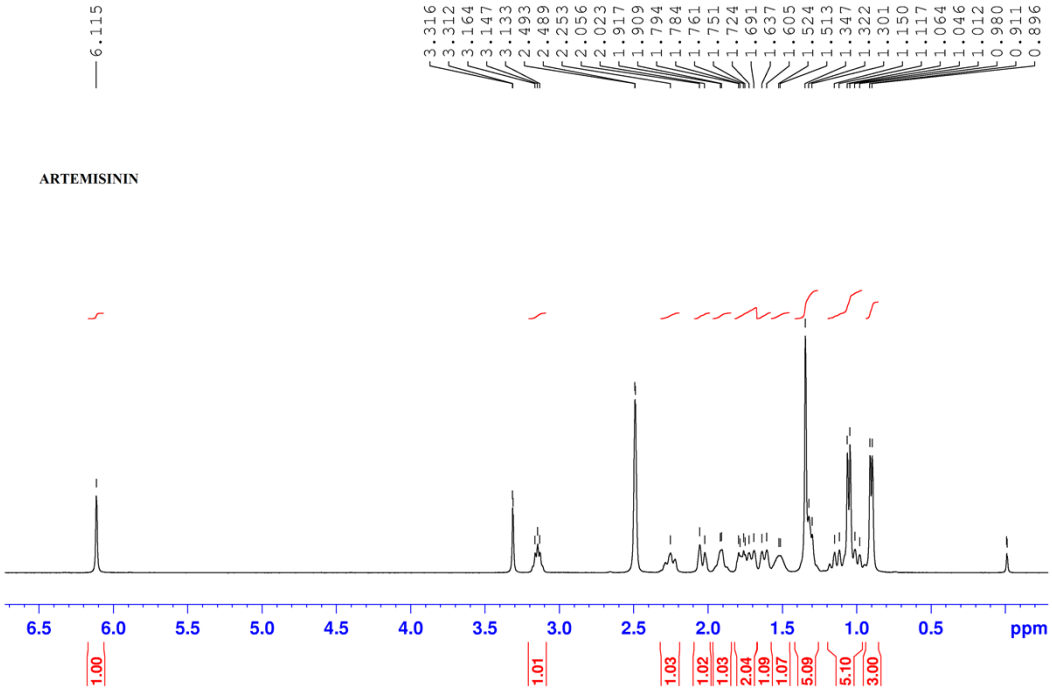


**Figure S3b** [1]H NMR spectrum of Artemisinin.

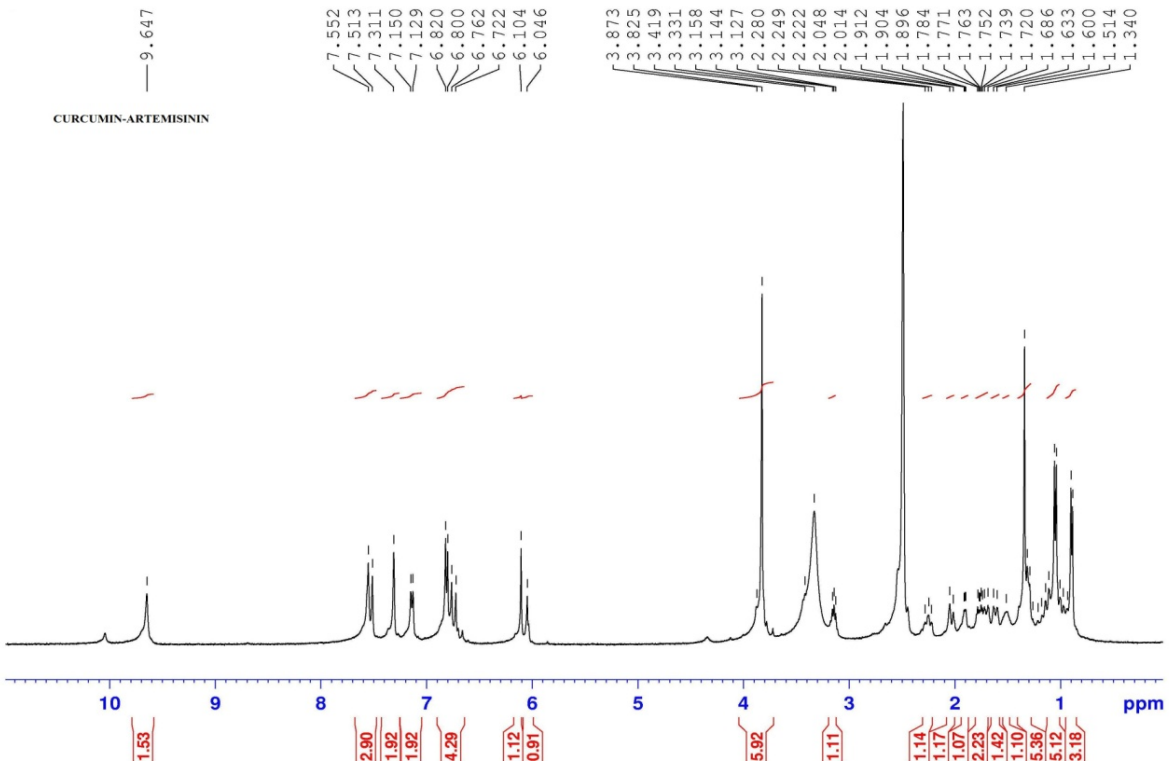


**Figure S3c** $^{1}$H NMR spectrum of Curcumin-Artemisinin is consistent with a 1:1 stoichiometry.

**Figure S3a-c** Proton NMR Spectra of CUR, ART and CUR-ART Coamorphous.

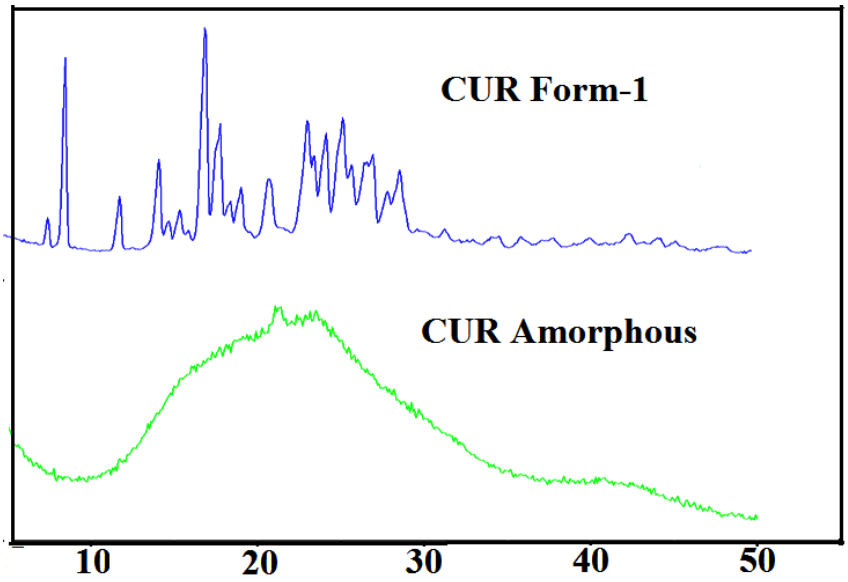


**Figure S4** PXRD pattern CUR crystalline and CUR amorphous forms obtained by rotavaporization.

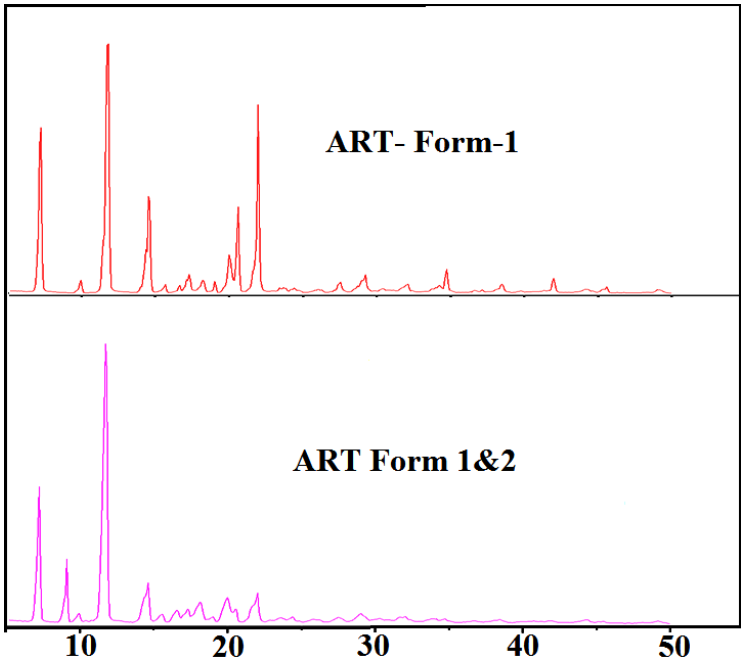


**Figure S5** PXRD pattern of ART Form 1 and mixture of ART Form 1 and 2 obtained by rotavaporization.

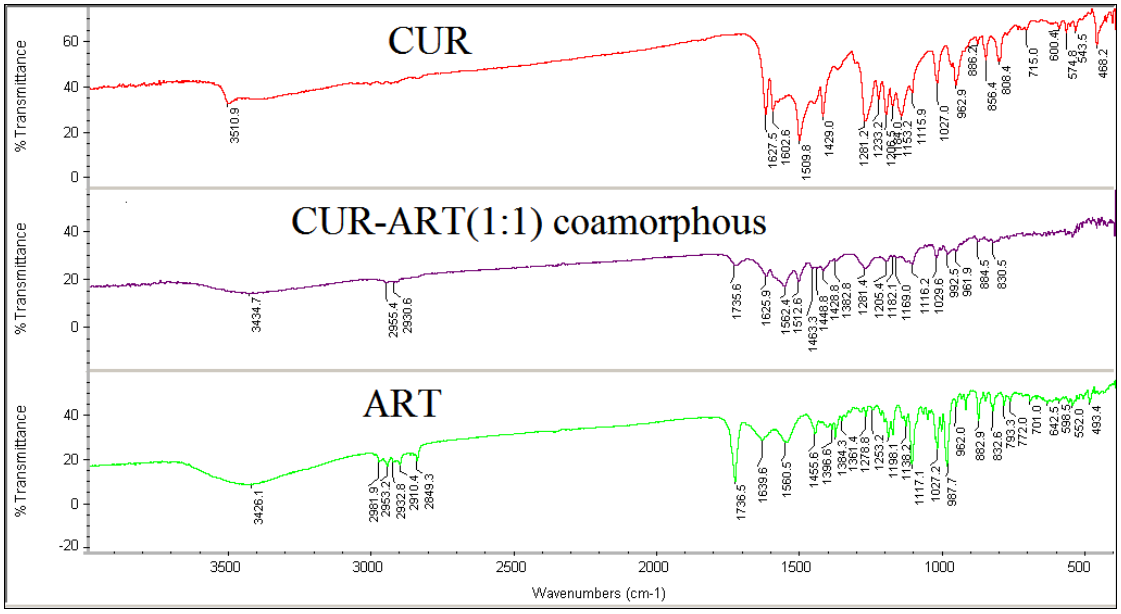


**Figure S6** Overlay of FT-IR spectra of CUR-ART coamorphous compared to the individual components

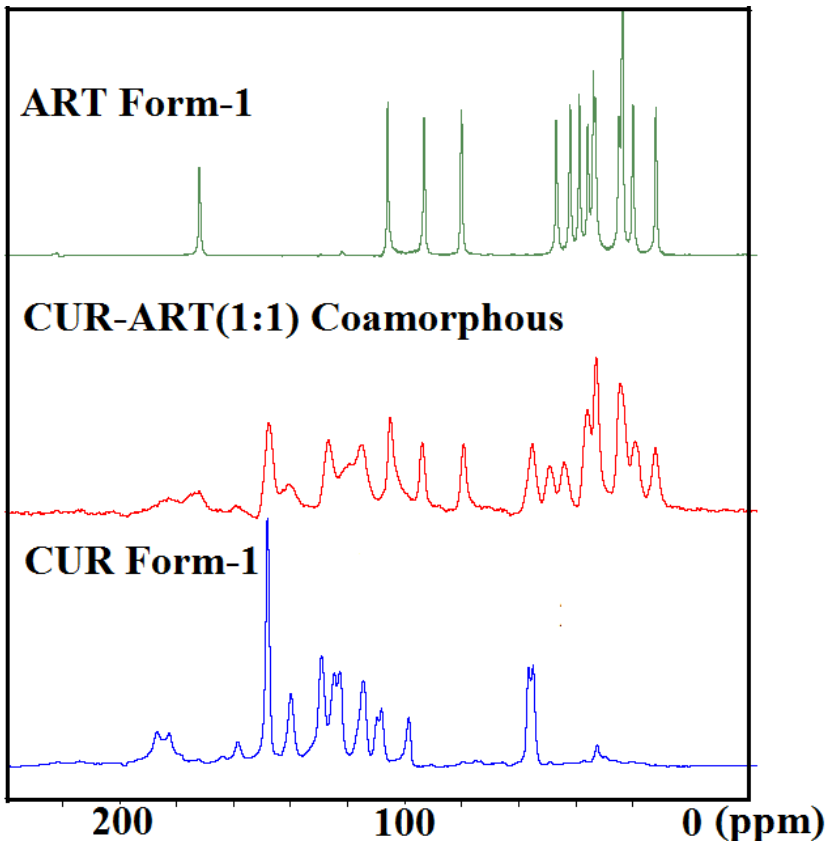


**Figure S7** Overlay of $^{13}C$ ss-NMR spectra of CUR-ART coamorphous compared to the individual components.

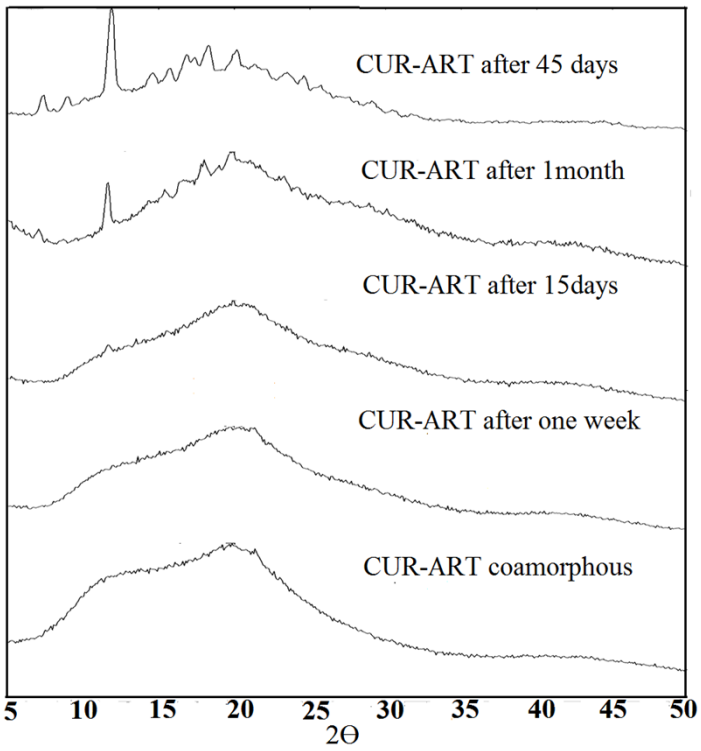


**Figure S8** PXRD plots CUR-ART kept in the stability chamber at 40 °C and 75% RH for 45 days.

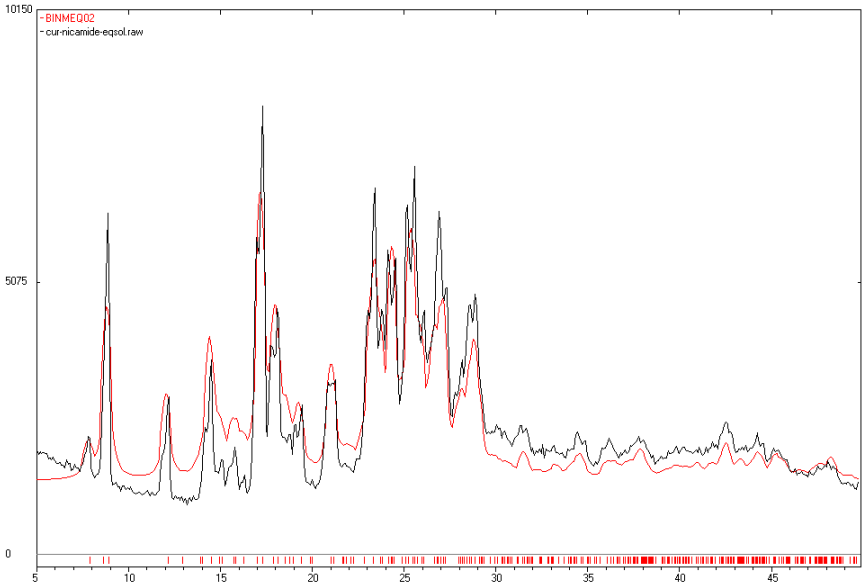


**Figure S9a** PXRD of CUR at the end of equilibrium solubility experiment matches with calculated XRD lines of curcumin form I.

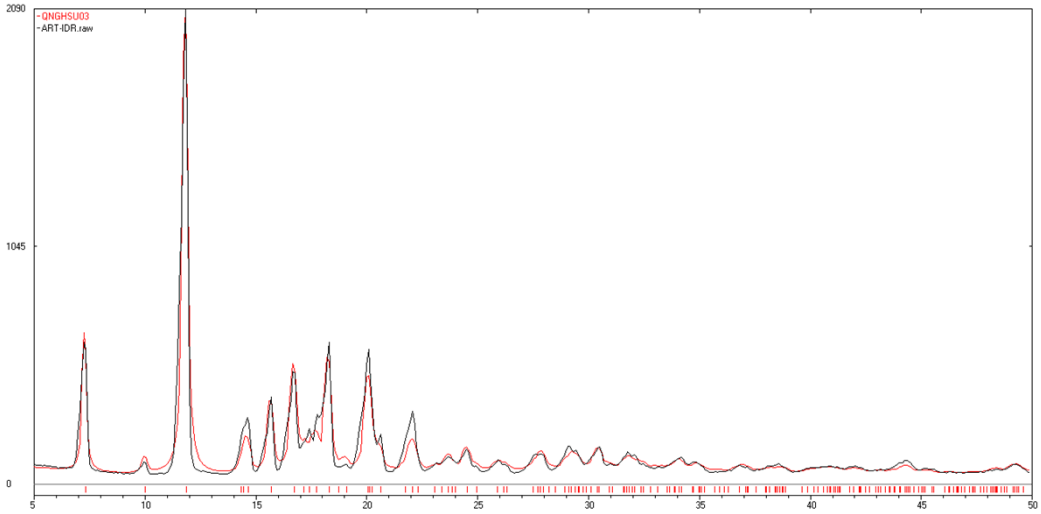


**Figure S9b** PXRD of ART at the end of equilibrium solubility experiment matches with calculated XRD lines of ART form I.

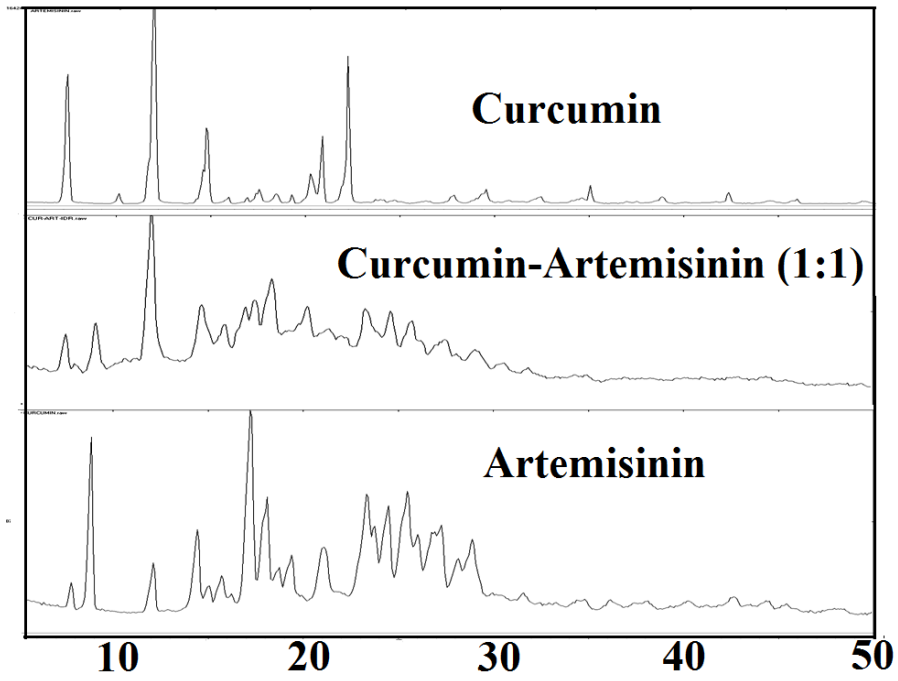


**Figure S9c** PXRD of CUR-ART coamorphous at the end of equilibrium solubility experiment matches with starting materials as a physical mixture of CUR and ART. The material at the end of solubility measurement is more crystalline compared to the grinding product shown in Figure S1 and S2. E.g. there are noticeable peaks after 2θ = 20°.

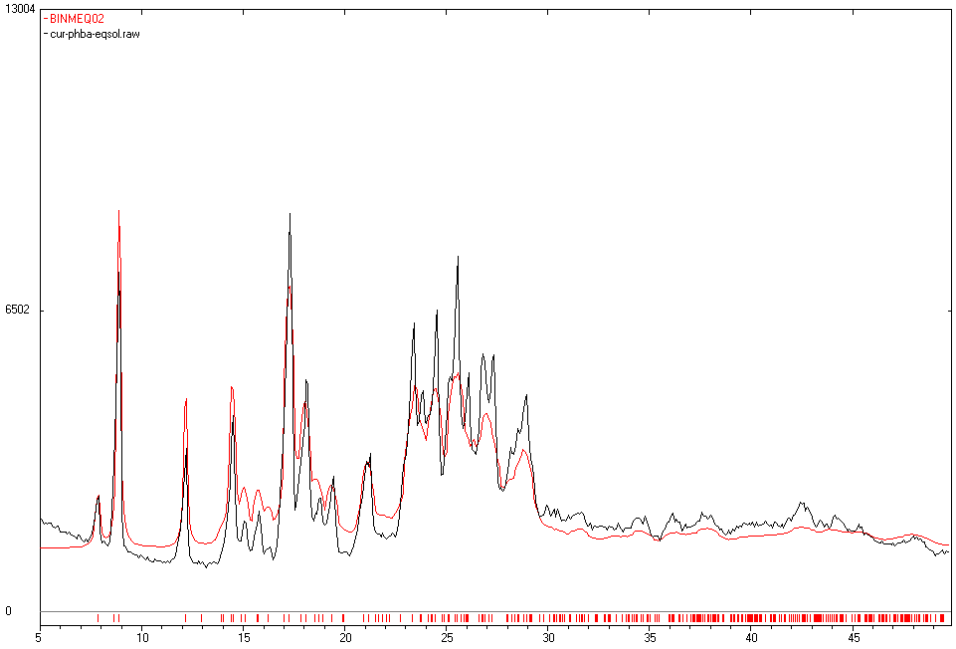


**Figure S9d** PXRD of CUR at the end of IDR experiment matches with calculated XRD lines of curcumin form I.

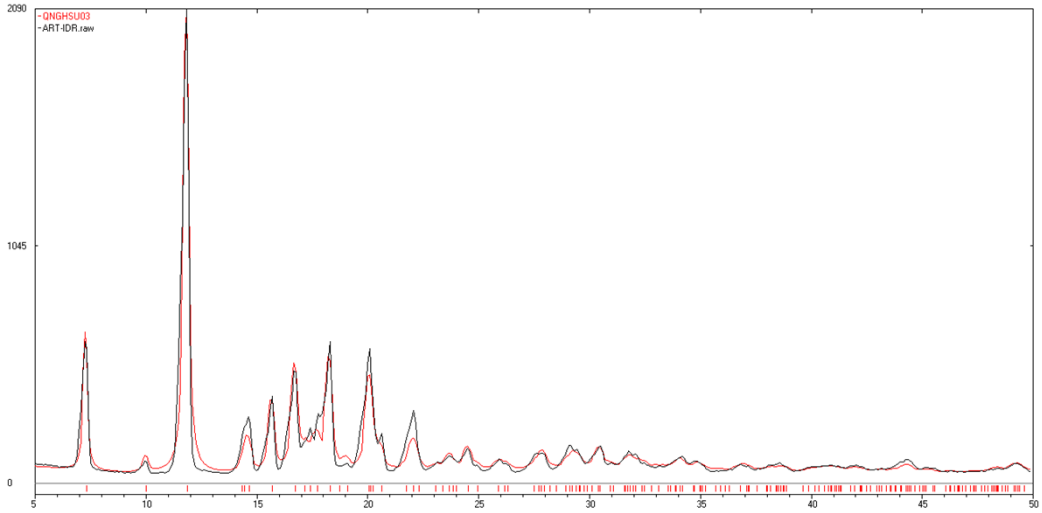


**Figure S9e** PXRD of ART at the end of IDR experiment matches with calculated XRD lines of ART form I.

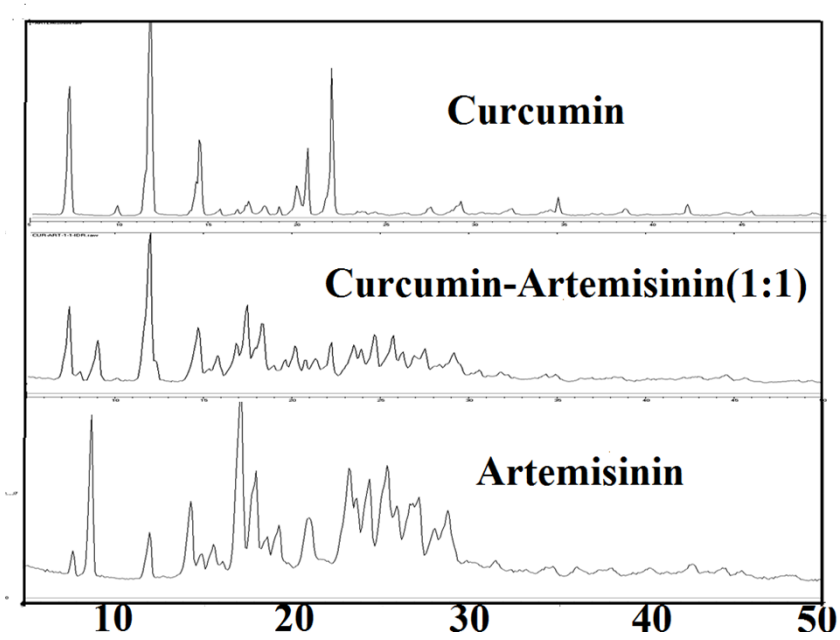


**Figure S9f** PXRD of CUR-ART coamorphous at the end of IDR experiment matches with starting materials like physical mixture of CUR-ART.

**Figure S9** Monitoring of CUR-ART form nature by PXRD after completion solubility and dissolution.

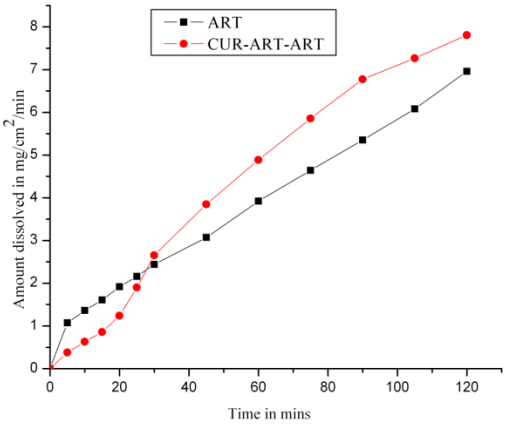


**Figure S10** ART and CUR-ART in 60% EtOH−$H_2O$.

**Table S1** Melting point, decomposition temperature, and phase transition point for CUR-ART coamorphous and their individual components (in °C).

| Sample name | Phase transition | Melting point | Decomposition point |
|---|---|---|---|
| CUR | -- | 181.42 | -- |
| CUR Amorphous | 98.90 | 170.93 | -- |
| ART | -- | 151.89<br>154.58 | 185.23 |
| CUR-ART | 67.58 | -- | 192.67 |

**Table S2** Intrinsic dissolution rates of CUR-ART coamorphous system in 60% EtOH−$H_2O$.[a,b]

| Compound | Molar Extinction coefficient ($mM^{-1}$ $cm^{-1}$) ($x10^6$) | Intrinsic dissolution rate, IDR ($mg/cm^2$)/min ($x10^{-3}$) | Cumulative amount dissolved per unit area (mg/L) |
|---|---|---|---|
| CUR | 100 | 0.177 | 17.01 |
| CUR-ART(1:1) Curcumin conc. | 200 | 0.461 (x2.6) | 41.31 (x2.4) |
| ART | 1 | 0.054 | 41.75 |
| CUR-ART(1:1) Artemisinin conc. | 2 | 0.043 (x1.2) | 46.84 (x1.1) |

[a] Curcumin and Artemisinin concentrations were determined by HPLC analysis.

[b] The amount of curcumin and artemisinin in samples for IDR was kept constant by taking molecular weights into account. CUR = 368, ART = 282 and CUR-ART (1:1) = 650.

**Experimental Section**

**Powder X-ray diffraction**

Powder X-ray diffraction was recorded on Bruker D8 Advance diffractometer (Bruker-AXS, Karlsruhe, Germany) using Cu-Kα X-radiation (λ = 1.5406 Å) at 40 kV and 30 mA power. X-ray diffraction patterns were collected over the 2θ range 5–50° at a scan rate of 5°/min.

**FT-IR Spectroscopy**

Nicolet 6700 FT-IR spectrometer with a NXR FT-Raman Module was used to record IR, NIR and Raman spectra. IR spectra were recorded on samples dispersed in KBr pellets.

**Solid-state NMR spectroscopy**

Solid-state $^{13}C$ NMR spectra were recorded on Bruker Avance 400 MHz spectrometer (Bruker- Biospin, Karlsruhe, Germany). ss-NMR spectra were carried out on a Bruker 4-mm double resonance CP-MAS probe in zirconia rotors with a Kel-F cap at 5.0-kHz spinning rate with a cross-polarization contact time of 2.5 ms and a delay of 8 s. $^{13}C$ NMR spectra were recorded at 100 MHz and referenced to the methylene carbon of glycine, and then recalibrated to the TMS scale ($\delta_{glycine}$ = 43.3 ppm).

**Thermal analysis**

Differential scanning calorimetry was performed on Mettler-Toledo DSC 822e module, (Mettler-Toledo, Columbus, OH). Samples were placed in crimped but vented aluminum pans for DSC experiments. The typical sample size was 3-5 mg for DSC. The temperature range for the thermogram was 30-300°C, and the sample was heated at a rate of 5 °C/min. Samples were purged in a stream of dry nitrogen flowing at 80 mL/min.

**Dissolution and solubility measurements**

The calculated molar extinction coefficients were used to determine the IDR values. For IDR measurements, 300 mg of the compound was taken in the intrinsic attachment and compressed to 0.5-$cm^2$ disk using a hydraulic press 4.0 ton/ $in^2$ pressure for 5 min. The intrinsic attachment was placed in a jar of 500 mL medium preheated to 37 °C and rotated at 150 rpm. 5 mL of the aliquot was collected at specific time intervals, and the concentration of the aliquots was determined with appropriate dilutions from the predetermined standard curves of the respective compounds. The IDR of the compound was calculated in the linear region of the dissolution curve (which is the slope of the curve or amount of drug dissolved/surface area of the disk) per unit time. The identity of the undissolved material after the dissolution experiment was ascertained by PXRD. The nature of the solid samples after disk compression and solubility and dissolution measurements were verified by PXRD.

**Chromatographic Conditions**

The HPLC analyses were performed using a Shimadzu Prominence model LC-20AD equipped with 20-mL injection loop, and a photodiode array detector. CUR was detected at 420 nm and ART at 210 nm. Data acquisition and analysis was carried out using LC solution software. A C18 reversed-phase column (250 mm × 4.6 mm, particle size 5 μm) preceded by a C18 guard column (33 mm × 4.6 mm) was used for analysis. In case of samples from in

vivo experiments, the mobile phase consisted of acetonitrile-5% acetic acid (75:25, v/v) and for IDR the mobile phase was acetonitrile-water (65:35 v/v). The mobile phase was run through the column at a flow rate of 1.0 mL/min.

**Animal study**

Sprague-Dawley rats (200±50g) were obtained from Sainath Agencies Limited (Hyderabad, India). Animals were acclimatized for 1 week prior to experimentation in a temperature-controlled, 12/12 hr light/dark room, and were allowed standard laboratory food and water. The rats were fasted overnight (~18 hr) with free access to water before the experiment. The study was conducted in compliance with standard animal use practices at Virchow Biotech Private Limited, Department of Preclinical Toxicology, Hyderabad, India (Registration No. 546/02/A/CPSCEA) and supervised by Dr. Durga Bhavani. This study was approved by Animal Ethics Committee meeting dated 6$^{th}$ January 2014.

**Liquid-Liquid extraction**

Coamorphous CUR-ART and CUR were extracted from plasma by deproteination. For each time-point, 0.4 mL of whole blood was collected from Retro orbital vein of rat eye into pre-chilled (4$^0$C) lithium heparin tube and placed on ice. Within 10 min of collection, blood samples were centrifuged at 2000g for 15 min at 4 °C. The resulting plasma was frozen at –80 °C until analysis. 0.2 mL of plasma samples are combined with 0.2 mL $CH_3CN$ solvent. The solutions were cyclomixed and sonicated in a bath sonicator for 10 min each followed by centrifugation for 15 min at 2000g. The supernatants were transferred into fresh eppendorf tubes and injected into the HPLC system.

**Pharmacokinetics study**

Pharmacokinetic studies of CUR-ART coamorphous and CUR were conducted in Sprague Dawley rats weighing (200±50 g) (n = 6) in cross-over design. Coamorphous CUR-ART and CUR (200 mg curcumin drug / kg of rat body weight) was suspended in 1% sodium carboxymethylcellulose and administered through oral gavage. Blood (0.4 mL) was withdrawn from retro-orbital plexus into lithium heparin tube at the following times after drug administration: 30, 45, 60, 90, 120, 180, 240, 360, 480 and 720 min. After centrifugation for 2000g for 15 min, an aliquot of 0.2 mL plasma was collected and analyzed by HPLC. Areas under the curve concentration (AUC in serum) vs. Time plots were calculated by the linear trapezoidal rule. The maximum plasma concentration, $C_{max}$, and the time $T_{max}$ required to reach $C_{max}$ were obtained from the plasma concentration curve.

**FESEM analysis**

Morphology and size of the micro structures of CUR, ART, CUR-ART coamorphous and CUR-ART physical mixture solid samples were examined on Carl Zeiss Field Emission Scanning Electron Microscope Model 6027 with MERLIN compact using a beam voltage of 5 kV.